Four-wave Mixing Response of a Graphene Layer Covered on a Tapered Fiber

Jiamei Lu, Qiang Jin, Xibin Li, Qiang Yan, Qianyu Gao, and Shiming Gao
Centre for Optical and Electromagnetic Research
State Key Laboratory of Modern Optical Instrumentation
Zhejiang University, Hangzhou 310058, China

Abstract— The nonlinear optical response of four-wave mixing (FWM) in a graphene layer covered on a tapered fiber is numerically investigated. The required graphene length is optimized to realize the maximum conversion efficiency, which is both affected by the incident power and propagation loss. Analysis shows that the graphene length is very short due to the heavy absorption in graphene, and the structure exhibits ultrabroad bandwidth. A conversion bandwidth of more than 300 nm is achieved with a conversion efficiency of more than −30 dB in a wide wavelength range of 0.8–1.8 μm.

1. INTRODUCTION

Nonlinear optical materials are always expected to be of smaller size and higher nonlinear coefficient. Graphene, which is of a single atomic layer thickness and whose nonlinear coefficient is five orders higher than silicon [1], has the potential to be an ideal ultra-compact nonlinear material. Resent experiments have observed higher harmonics generation [2], nonlinear self-focusing [3], and four-wave mixing (FWM) [4, 5] phenomena in graphene. Since graphene is a very thin film, it is reasonable to be composed with other materials or devices, such as tapered fibers, to extend the interaction length with the optical field. When a graphene layer is covered on a tapered fiber, a large portion of light propagates outside the fiber via evanescent field if the core radius is small enough. Such a structure is expected to extend the interaction distance and enhance the nonlinear effect. Gorbach et al has tried to analyze the nonlinear property and loss in a graphene-clad tapered fiber [6], but the four-wave mixing response in such a structure is not studied yet. In this paper, we theoretically analyze the FWM effect in a graphene layer covered on a tapered fiber, whose structure is shown in Fig. 1. The structure length is optimized to obtain maximum conversion efficiency at different wavelengths. The bandwidth property is analyzed at a fixed waveguide length. At last, the nonlinear response of the graphene layer on a tapered fiber is compared to that of a pure tapered fiber.

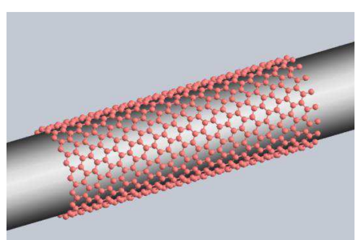

Figure 1: Schematic description of a graphene layer covered on a tapered fiber.

2. THEORETICAL ANALYSIS

When a pump ω_P and a signal ω_S are injected into a graphene layer covered on a tapered fiber, the total field is expressed as

$$E = \frac{1}{2} \sum_{j=P,S,I} E_j \exp\left[i\left(\beta_j z - \omega_j t\right)\right] + c \cdot c. \tag{1}$$

For the FWM process to generate the idler ω_I ($\omega_I = 2\omega_P - \omega_S$), the nonlinear response is

$$D(\omega_I) = \varepsilon_0 \varepsilon E(\omega_I) + \varepsilon_0 \chi^{(3)} \vdots E(\omega_P) E^*(\omega_P) E(\omega_S) \tag{2}$$

where ε is the relative permittivity and $\chi^{(3)}$ is the third-order susceptibility tensor, which corresponds to graphene or silica for different locations on the transverse cross section. For the graphene layer, the relative permittivity ε $(= \varepsilon_g)$ can be obtained from its dynamical conductivity using Kubo formula $\sigma_g = \sigma_{inter} + \sigma_{intra}$ [7], where the interband and intraband contributions are

$$\sigma_{intra}(\omega) = \frac{je^2\mu}{\pi\hbar^2(\omega + j\tau^{-1})} \tag{3}$$

$$\sigma_{inter}(\omega) = \frac{je^2}{4\pi\hbar}\ln\left(\frac{2|\mu| - (\omega + j\tau^{-1})\hbar}{2|\mu| + (\omega + j\tau^{-1})\hbar}\right) \tag{4}$$

where μ is chemical potential and τ is the relaxation time. Supposing that the thickness of graphene layer is Δ, one can obtain the relative permittivity:

$$\varepsilon_g \equiv \frac{i\sigma_g}{\varepsilon_0\omega\Delta} + 1 \tag{5}$$

According to the permittivity distribution of the composited structure, one can get the mode field distribution and the effective refractive index denoted as $n_{eff} = n(1 - iK)$. The linear phase mismatch can be got from the real part of the effective refractive, which is $\Delta\beta = 2\pi(n_S/\lambda_S + n_I/\lambda_I - 2n_P/\lambda_P)$ for the FWM process $\omega_I = 2\omega_P - \omega_S$. And the imaginary part represents the linear absorption of the structure. Considering the saturation absorption property and two-photon absorption (TPA) [8, 9] of graphene, the total propagation loss can be obtained as $\alpha = \alpha_0/(1 + I/I_S) + \beta_{TPA}I$, where I is the incident intensity, Is is the saturation irradiance, $\alpha_0 = 2\omega(nK/c)$ represents the linear loss, and β_{TPA} is the TPA coefficient.

Substituting Eq. (2) to Maxwell's curl equations for the electric and the magnetic fields, one can get the coupled wave equations for degenerate FWM:

$$\begin{aligned}&\frac{\partial A_P}{\partial z} + \beta_{1P}\frac{\partial A_P}{\partial t} + \frac{i}{2}\beta_{2P}\frac{\partial^2 A_P}{\partial t^2} + \frac{1}{2}\alpha_P A_P \\ = \ & i\gamma_P\left(|A_P|^2 + 2|A_S|^2 + 2|A_I|^2\right)A_P + 2i\gamma_P A_P^* A_S A_I \exp(i\Delta\beta z)\end{aligned} \tag{6}$$

$$\begin{aligned}&\frac{\partial A_S}{\partial z} + \beta_{1S}\frac{\partial A_S}{\partial t} + \frac{i}{2}\beta_{2S}\frac{\partial^2 A_S}{\partial t^2} + \frac{1}{2}\alpha_S A_S \\ = \ & i\gamma_S\left(|A_S|^2 + 2|A_P|^2 + 2|A_I|^2\right)A_S + i\gamma_S A_I^* A_P^2 \exp(-i\Delta\beta z)\end{aligned} \tag{7}$$

$$\begin{aligned}&\frac{\partial A_I}{\partial z} + \beta_{1I}\frac{\partial A_I}{\partial t} + \frac{i}{2}\beta_{2I}\frac{\partial^2 A_I}{\partial t^2} + \frac{1}{2}\alpha_I A_I \\ = \ & i\gamma_I\left(|A_I|^2 + 2|A_P|^2 + 2|A_S|^2\right)A_I + i\gamma_I A_S^* A_P^2 \exp(-i\Delta\beta z)\end{aligned} \tag{8}$$

In the graphene covered on a tapered fiber, the nonlinearities of graphene and silica are quite different. As a result, nonlinear parameters $\gamma_{P,S,I}$ should identify the local field corresponding to what kind of materials, which can be obtained by using a common expression [10]:

$$\gamma = \frac{3\omega}{4}\varepsilon_0 \frac{\iint \chi^{(3)}(x,y)\left|\vec{E}\right|^4 dxdy}{\left|\iint_{D_{total}} \mathrm{Re}\left\{\vec{E} \times \vec{H}^*\right\} \cdot \hat{e}_z dxdy\right|^2} \tag{9}$$

where E and H^* are the distribution of the electric field and the conjugate of magnetic field, and $\hat{e}_z$ is the unit vector along the propagation direction. In Eq. (9), $\chi^{(3)}(x,y)$ represents the third-order susceptibility of graphene or silica due to the material that the micro area corresponds to.

To evaluate the FWM response in the graphene on a tapered fiber, the conversion efficiency can be defined as the ratio of the generated idler power with respect to the incident signal power:

$$\eta = |A_I(L)|^2 / |A_S(0)|^2 \tag{10}$$

By numerically solving Eqs. (6)–(8), the output idler $A_I(L)$ and hence the conversion efficiency can be obtained.

3. SIMULATION AND ANALYSIS

By setting $\mu = 0.02\,\mathrm{eV}$ and $\tau = 5 \times 10^{-13}\,\mathrm{s}$ for graphene, and adopting the diameter of the tapered fiber as $0.7\,\mu\mathrm{m}$, the nonlinear parameter of the composite structure is calculated from the electric field distribution along with the linear absorption and the total loss involving both linear and TPA losses, as shown in Fig. 2(a). One can find that graphene greatly enhances the nonlinear parameter, but meanwhile a large loss is brought. In particular, the wavelengths for higher nonlinear parameters also suffer from higher losses because more electric field is restricted in the graphene layer. Fig. 2(b) shows the conversion efficiency as a function of graphene length using a pump whose pulse peak power is 10 W, pulse width is 100 ps, and wavelength is set to be 1.3, 1.5, or $1.7\,\mu\mathrm{m}$ (signal wavelength is approximately equal to the pump wavelength), respectively. From Fig. 2(b), one can find that different graphene lengths are needed to reach their maximum conversion efficiency for different pump wavelengths. The required graphene length and the corresponding maximum conversion efficiency are plotted in Fig. 2(c). Although the required graphene lengths are different for various wavelengths, they are all as short as few ten micrometers. The maximum conversion efficiency reaches $-23.5\,\mathrm{dB}$ when the pump wavelength is $1\,\mu\mathrm{m}$. A short wavelength needs a short length to reach the maximum efficiency due to its high nonlinear parameter and heavy loss, and the peak efficiency is higher than that of longer wavelength.

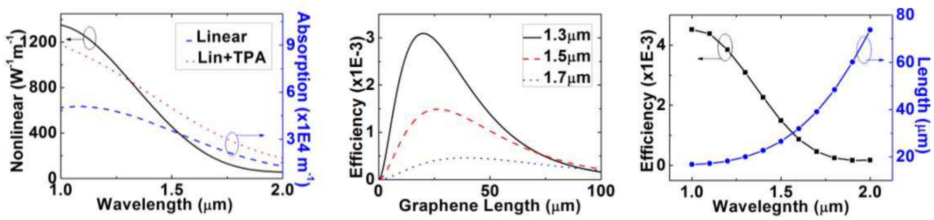

(a) (b) (c)

Figure 2: (a) Nonlinear parameter, linear absorption, and total absorption. (b) Conversion efficiency along the graphene length. (c) Optimized graphene length and the corresponding maximum conversion efficiency.

Since the required graphene layer is quite short, it is expected to have ultrabroad conversion bandwidth. Assuming the graphene length is $30\,\mu\mathrm{m}$, Figs. 3(a) and 3(b) show the nonlinear phase shift κL, where L is the graphene length and $\kappa = (\Delta\beta + 2\gamma P_P)$ is the total phase mismatch, and the corresponding conversion efficiency as the signal wavelength varies, pumped by 0.8-, 1.3-, and 1.8-μm lights, respectively. The signal and converted idler wavelengths are set to be within $2.4\,\mu\mathrm{m}$ because the structure no longer constrains longer wavelength to form guide mode. As nonlinear parameter is rapidly enhanced as the wavelength shortens, which means a high efficiency for the conversion from long-wavelength signal to short-wavelength idler, the maximum conversion efficiency emerges at signal wavelength longer than pump wavelength. Fig. 3(c) shows the bandwidth and maximum efficiency at different pump wavelengths. It turns out that owing to graphene, the waveguide has an ultrabroad bandwidth about from 315 to 720 nm with maximum conversion efficiency about from -23.7 to $-27.8\,\mathrm{dB}$ as the pump wavelength varies from 0.8 to $1.8\,\mu\mathrm{m}$. The bandwidth is related to the dispersion of the structure, as shown in Fig. 3(d). The zero dispersion wavelength (ZDW) emerges in $0.89\,\mu\mathrm{m}$, which corresponds the broadest bandwidth of 720 nm in Fig. 3(c).

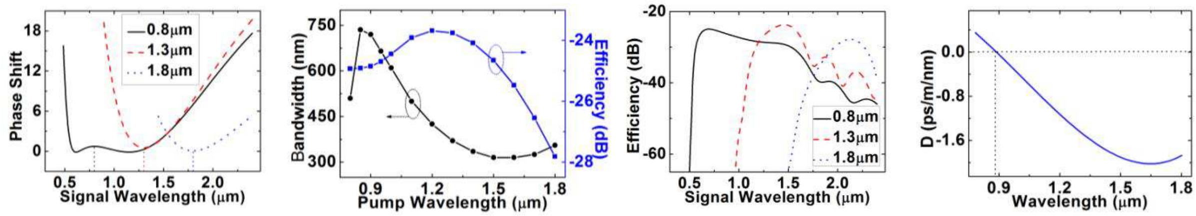

(a) (b) (c) (d)

Figure 3: (a) Nonlinear phase shift and (b) conversion efficiency as the signal wavelength varies. (c) Bandwidth and the maximum conversion efficiency at different pump wavelengths. (d) Dispersion value of the structure as the wavelength varies.

For comparison, we also simulate the nonlinear optical response in a pure tapered fiber. The obtained nonlinear coefficient of the pure tapered fiber with the same dimensions is shown in Fig. 4(a), which is three orders smaller than graphene cover one. In order to reach the same conversion efficiency as grapheme layer on the tapered fiber (-24.6 dB with a 1.5-μm pump), the pure tapered fiber length is set to be 10 cm. Figs. 4(b) and 4(c) show the nonlinear phase shift and the corresponding conversion efficiency for the pure tapered fiber pumped by a 1.5-μm light, whose pulse peak power is also 10 W and pulse width is 100 ps. The FWM bandwidth of the pure tapered fiber is calculated to be only 8.6 nm, which is much narrower than the graphene layer covered one since it needs to propagate much longer distance to attain the same conversion efficiency.

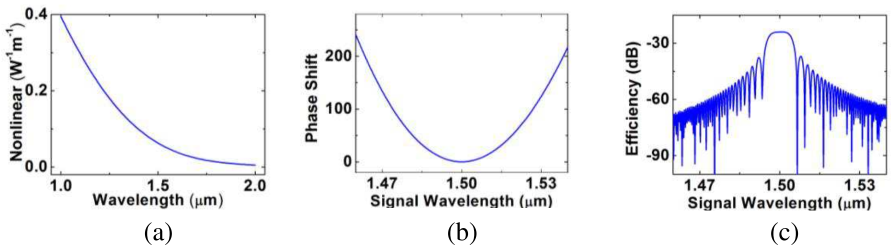

Figure 4: (a) Nonlinear parameter of pure tapered fiber. (b) Nonlinear phase shift and (c) conversion efficiency as the signal wavelength varies in the pure tapered fiber.

4. CONCLUTIONS

FWM are theoretically analyzed in a graphene layer covered on a tapered fiber considering the nonlinear parameter for composite structures. The graphene length is optimized to obtain maximum conversion efficiency at different pump wavelengths. Due to the ultrashort grahene length, such a composite structure shows the performance of ultrabroad bandwidth. A conversion bandwidth of more than 300 nm is achieved with a conversion efficiency of more than -30 dB in a wide wavelength range of 0.8–1.8 μm. By comparing with the pure tapered fiber without graphene, the composite structure shows much broader bandwidth to get the same conversion efficiency since much shorter interaction length is used.

ACKNOWLEDGMENT

This work was supported by the Specialized Research Fund for the Doctoral Program of Higher Education of China (Grant No. 20130101110089), the National Natural Science Foundation of China (Grant No. 61178001), and the Zhejiang Provincial Natural Science Foundation of China (Grant No. LY14F050006).

REFERENCES

1. Hendry, E., P. J. Hale, J. Moger, A. K. Savchenko, and S. A. Mikhailov, "Coherent nonlinear optical response of graphene," *Phys. Rev. Lett.*, Vol. 105, No. 9, 097401, 2010.
2. Dean, J. J. and H. M. van Driel, "Graphene and few-layer graphite probed by second-harmonic generation: Theory and experiment," *Phys. Rev. B*, Vol. 82, No. 12, 125411, 2010.
3. Gorbach, A. V., "Nonlinear graphene plasmonics: Amplitude equation for surface plasmons," *Phys. Rev. A*, Vol. 87, No. 1, 013830, 2013.
4. Gu, T., N. Petrone, J. F. McMillan, A. van der Zande, M. Yu, G. Q. Lo, D. L. Kwong, J. Hone, and C. W. Wong, "Regenerative oscillation and four-wave mixing in graphene optoelectronics," *Nat. Photonics*, Vol. 6, No. 8, 554–559, 2012.
5. Wu, Y., B. Yao, Y. Cheng, Y. Rao, Y. Gong, X. Zhou, B. Wu, and K. S. Chiang, "Four-wave mixing in a microfiber attached onto a graphene film," *IEEE Photon. Technol. Lett.*, Vol. 26, No. 3, 249–252, 2014.
6. Gorbach, A. V., A. Marini, and D. V. Skryabin, "Graphene-clad tapered fiber: Effective nonlinearity and propagation losses," *Opt. Lett.*, Vol. 38, No. 24, 5244–5247, 2013.
7. Vakil, A. and N. Engheta, "Transformation optics using graphene," *Science*, Vol. 332, No. 603m5, 1291–1294, 2011.
8. Yang, H., X. Feng, Q. Wang, H. Huang, W. Chen, A. T. S. Wee, and W. Ji, "Giant two-photon absorption in bilayer graphene," *Nano Lett.*, Vol. 11, No. 7, 2622–2627, 2011.

9. Li, W., B. Chen, C. Meng, W. Fang, Y. Xiao, X. Li, Z. Hu, Y. Xu, L. Tong, H. Wang, W. Liu, J. Bao, and Y. R. Shen, "Ultrafast all-optical graphene modulator," *Nano Lett.*, Vol. 14, No. 2, 955–959, 2014.
10. Koos, C., L. Jacome, C. Poulton, J. Leuthold, and W. Freude, "Nonlinear silicon-on-insulator waveguides for all-optical signal processing," *Opt. Express*, Vol. 15, No. 10, 5976–5990, 2007.